EFFECTS OF LAND COVER CHANGE ON THE HYDROLOGIC REGIME OF KABOMPO RIVER BASIN, ZAMBIA

J.M. Kampata [1,2], T.H.M Rientjes [1], J. Timmermans [2]

[1] *Department of Water Resources, Faculty of Geo-information Science and Earth Observation (ITC) University of Twente, P.O. Box 6, 7500AA, Enschede, The Netherland. Email:j.m.kampata@utwente.nl*
[2] *Department of Water Affairs, Ministry of Mines, Energy and Water Development, P.O Box 50288, Lusaka. Zambia. Email:jkampata@yahoo.com*

ABSTRACT

Over the past decades, the Kabompo River Basin in Zambia is affected by deforestation and land degradation as a consequence of intensified agriculture and mining. Changes presumably have affected the hydrological catchment behaviour and related seasonal flow regimes. Impact assessments are unknown for the basin.

In this study multi-decadal time series of rainfall and stream flow were evaluated by trend analysis, change point detection methods and analysis on high and low flow exceedance probabilities. Results are combined with satellite based land cover observations for 1984, 1994, 2001 and 2009. Unsupervised classification of the Landsat images indicate pronounced land cover changes. Preliminary results of this study show that i) precipitation time series are not directly affected by climate change and ii) changes in stream flow can be linked to changes in land cover.

1. INTRODUCTION

In many African catchments, sustainability of water resources is under threat due to changes in land cover and our climate. Changes in land cover directly impact the catchment runoff behavior and consequently the seasonal runoff regime. Changes in land cover commonly are diffusive in the time domain making hydrological impacts assessments complicated. Well know examples of land cover changes are deforestation due to agriculture expansion but also land degradation by poor agricultural practices, tillage and ultimately erosion. Principle to such changes is that any change in land cover directly affects hydrological responses although such is not directly quantifiable at catchment scale by issues of smoothing of small scale responses. Examples of hydrological impacts by land cover changes at local scale are, increased evaporation, reduced recharge, increased infiltration whereas at catchment scale such may result in e.g. reduced low flows, more frequent high flow events with possibly increased peak flows, more frequent inundation, and changes in seasonal runoff volumes., Although land cover changes interrelate to hydrological impacts, research findings on interrelations are inconsistent [1].

Moreover, assessments often are intricate by issues of climate change, poor data availability, and lack of accurate land cover data. Such particularly applies to less developed countries were resources are limited.

Alternative to the use of ground based (i.e., field measured) data is the use of satellite remote sensing. Advances in satellite remote sensing (RS) has helped to overcome limitations by poor data availability because of low density observation networks. It is often advocated that assessments on hydrological impacts by land cover changes would benefit from availability of RS data. Also, RS data could serve to improve parameterisation of hydrological models such as rainfall-runoff models. However, prior to use of hydrological models, statistical analysis on rainfall and stream flow at gauges stations should be undertaken to investigate if the flow regime (indeed) is affected.

The focus of this paper is access the effects of land cover change on stream flow in the Kabompo River Basin. In this study statistical tests on trends in rainfall and stream flow, and analysis of land cover using satellite remote sensing techniques and hydrological modelling is practised.

2. STUDY AREA AND DATA SOURCES

The Kabompo River Basin is located between between Latitudes 11^0S and 15^0S, Longitudes 23^0E and 26^0E in Northwestern part of Zambia. The Kabompo River is a tributary to the Zambezi River with its source in the North-Western Province of Zambia along the watershed between the Zambezi and Congo River basins. The Kabompo river basin has an area of 72,140 km^2. The gauging station at Kabompo River at Watopa Pontoon which is near the basin outlet has an upstream area of area of 67,261 km^2. Fig. 1 shows the location of the Kabompo River Basin. Hydrological and Meteorological Stations are indicated.
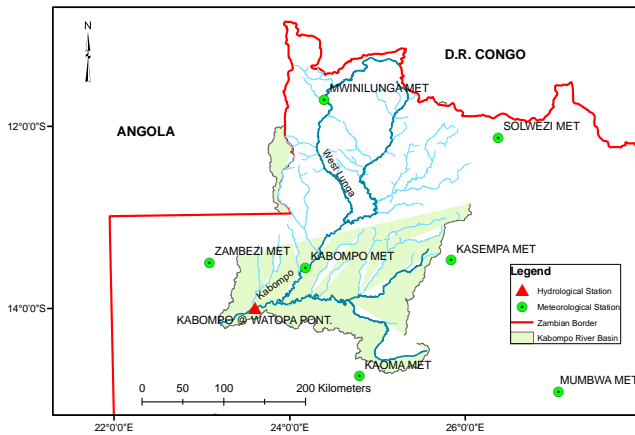
Figure 1. Location of the Kabompo River Basin.

The study area experiences three distinct seasons of Wet and hot (November to March), Dry and cool (April to July) and Dry and hot (August to October). The mean annual potential evapotranspiration (ETp) is 1337mm and mean annual rainfall is 1200mm [2].

Stream flow data was obtained for the hydrological station, Kabompo River at Watopa Pontoon, from the Zambezi River Authority and Department of Water Affairs in Zambia. Rainfall data was collected from the Meteorological Department. The stations Mwinilunga, Solwezi, Zambezi and Kabompo were found to have long term consistent data. The daily and monthly stream flow and rainfall data covered the hydrological years from 1973 to 2010. The hydrological year covers the period 1st October to 30th September.

The study area is covered by six Landsat images in path 174 to 175 and rows 68, 69 and 70. The Landsat images with surface reflectances corrected for atmospheric effects were obtained from the United States Geological Survey (USGS) (http://earthexplorer.usgs.gov/) for the years 1984, 1994, 2001 and 2009. The Landsat surface reflectance images are generated using the Landsat Ecosystem Disturbance Adaptive Processing System (LEDAPS) processor [3]. They are from the Landsat Surface Reflectance Product (LSRP) which is available since May 2013. In total 24 satellite images were obtained. The images were selected based on the following criteria: (a) A cloud cover of less than 10% as this is most suited for image classification; (b) images should be available for the dry season as agriculture plots can be best distinguished, (c) Anniversary dates should be such that change due to seasonality and phenology differences are minimal and (d) Images along one path should be available for the same day.

3. METHODOLOGY

3.1 Land cover classification

For land cover classification (LCC) in this study, Landsat 5 Thematic Mapper (TM) satellite imagery from 1984, 1994, and 2009 was used as well as images from the Landsat 7 Enhanced Thematic Mapper (ETM+) image for the year 2001.

Satellite images were obtained already processed to L1T. Images were set to the UTM map projection Zone 35S; Reference datum and Reference Ellipsoid WGS84. The 2009 images were taken as the base images. To verify co-registration, each image date was checked against the 2009 corresponding images using image to image registration. A root mean square error (RMSE) < 0.5 was targeted. The 3 images along the same path acquired on the same day were mosaicked prior to classification. Unsupervised classification was performed using the ISODATA algorithm [4] for 15 and 25 classes. A comparison of the two classifications was made and Regions of Interest (ROIs) that in a second classification stage were used to improve classification by use of identified classes that did not change. By lack of ground truth (i.e., field survey data), the ROIs collected are considered to be surrogates of actual ground control points. For this, we used Google Earth maps, we visually interpreted the respective images and we used our own knowledge of the area to identify the various classes. This resulted in six classes namely: (i) Evergreen Forest (EF), (ii) Deciduous Forest (DF), (iii) Savanna and grassland (SA), (iv) Agriculture and Bare land (AG); (v) Water (WA) and (vi) Wetlands (WL). This was followed by supervised classification using the Maximum Likelihood Classifier.

Using Hawth's Analysis Tools for ArcGIS [5], 200 points were randomly generated covering the study area. These were used to identify pixels that only overlay one type of land cover where a nearby suitable identified area was used to collect pixels for the ROI. Additional ROIs were also defined using polygons and scatter plots to collect samples for land cover types such as water, wetland and agriculture land that were not adequately captured by the random samples. The ROI where identified after ensuring that the land cover was stable by ensuring that it was the same in the unsupervised classified of 15 classes and that of 25 classes. The defined ROIs were used as training points in the supervised classification. To ensure consistency in classification, the same training samples collected on the overlap area (Fig. 2) were used when classifying each image. This was in addition to other training samples in other areas of the image. The resulting classifications were then mosaicked. Further, accuracy of classification was quantitatively assessed using the confusion matrix [6]. The reference data ("ground truth

data") was collected by visual interpretation of the satellite image using the generated random points as a guide of location where the data was obtained. This was done for each set of mosaicked images for each year. Data processing software used was ENVI 5.0, ArcGIS 10.1 and MS Excel.
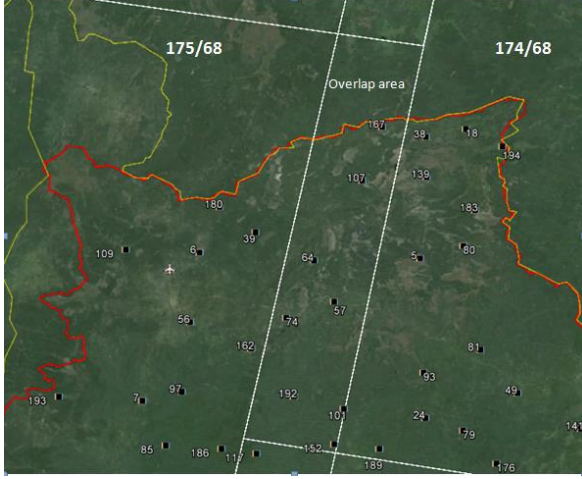

Figure 2. Landsat footprint over a Goggle Earth image showing ROIs data collection points and overlap areas for scenes 175/68 and 174/68

3.2   Trends in rainfall and stream flow

The Mann- Kendall test for trend analysis was applied to the annual and monthly rainfall data for the Kabompo River basin to assess if rainfall is affected by climate change. The Mann Kendall Test is a non- parametric test that is widely used for detecting monotonic (gradual) trends in hydrologic variables [7]. The Mann-Kendall statistic S is computed as:

$$S = \sum_{k=1}^{n-1} \sum_{j=k+1}^{n} \text{sgn}\left(x_j - x_k\right) \qquad (1)$$

Where:

$$\text{sgn}\left(x_j - x_k\right) = 1 \quad \text{if } x_j\text{-}x_k > 0 \qquad (2)$$
$$= 0 \text{ if } x_j\text{-}x_k = 0$$
$$= -1 \text{ if } x_j\text{-}x_k < 0$$

The variance of S was computed as:

$$VAR(S) = \frac{n(n-1)(2n+5) - \sum_t t(t-1)(2t+5)}{18} \qquad (3)$$

Where: n is the number of data points and t the number of data in a given tie. Ties are the equal data values in a time series when the data is ranked.

Then S and VAR(S) were used to compute the test statistic Z as:

$$Z = \frac{S-1}{VAR(S)^{1/2}} \qquad \text{if } S > 0 \qquad (4)$$

$$= 0 \qquad \text{if } S = 0$$

$$= \frac{S+1}{VAR(S)^{1/2}} \qquad \text{if } S < 0$$

A positive value of S indicates that there is an increasing trend and a negative value indicates a decreasing trend. The null hypothesis (H_0) for the test is that the trend is not significant. The Z-statistic (test statistic) is calculated and evaluated against critical test statistic ($z_{\alpha/2}$) values for the chosen level of significance. The Mann-Kendall test was conducted at the 5% significance level (α =0.05) (i.e. $Z_{0.025}$=1.96).

If the absolute value of the calculated Z-statistic is less than the significance level at α (alpha) = 0.05, the H_0 is accepted. Rejecting H_0 indicates that a trend s significant.. The rate of change of trend is calculated using the Sen slope estimator [8]. The analysis was done using the Computer program for the Kendall family of trend tests [8]) as well as in MATLAB using script developed by [9].

3.3   Change detection of stream flow

Change detection in the stream flow time series was investigated using the moving t-test (MTT) technique following the procedure used by [1]; [10]; [11]. The MTT considers if the difference in the mean of variables in adjacent time intervals reaches a stipulated statistical significance level. If it does, an abrupt change is inferred to have occurred [1].

The stochastic variable sequence of annual runoff is divided into two sub-sets, x_1 and x_2. Let μ_i, S_i^2 and n_i represent the mean, variance and sample size of the two sub-sets ($i = 1, 2$), respectively. The data are then analysed using the null hypothesis Ho: $\mu_1 = \mu_2$ and the test statistic, t_0, is calculated as [7]; [10]; [11]:

$$t_0 = \frac{\overline{\quad\quad\quad}}{\text{p}\sqrt{\left[\frac{}{\text{n}} \quad \frac{}{\text{n}}\right]}} \qquad (5)$$

$$S_p = \sqrt{\left[\frac{(n_1-1)S_1^2 + (n_2-1)S_2^2}{n_1+n_2-2}\right]} \qquad (6)$$

is the square root of the pooled sample variance (or pooled sample standard deviation). $n_1 = n_2 = N$ is taken for a N year moving average [1]. The degree of freedom (df) is given as $n_1 + n_2 - 2$. $n_i - 1$, known as the Bessel's correction, is used instead of n_i in the formula for the sample variance as it corrects the bias in the estimation of the population variance [12].For the analysis a significance level of α= 0.05 is selected for which the absolute value of the critical t-value, obtained from Critical Values of the t Statistic table, $t_\propto$ is obtained.

The null hypothesis *Ho* will be rejected for $|t_0| > |t_\propto|$. This would suggest that a variability in the time series is larger than the natural variability indicating aspects of climate change. Taking $n_1 = n_2 = 5$ (5 year moving average) and probability level *p = 0.05* with $n_1 + n_2 - 2 = 8$ degrees of freedom. The critical value of the

Student's t-distribution $t_\propto = 2.3$ is obtained from the Statistical Tables of Critical Values of the t Statistic [13].

To investigate how stream flow characteristics are varying in the periods that have statistically significant differences in the mean annual flows, the high flow (Q_5/Q_{50}) and low flow (Q_{95}/Q_{50}) indexes are estimated using the Weibull plotting position [1]; [14].

4. RESULTS

4.1 Land cover classification

Classified land cover maps for1984, 1994, 2001 and 2009 are shown in Fig. 3.
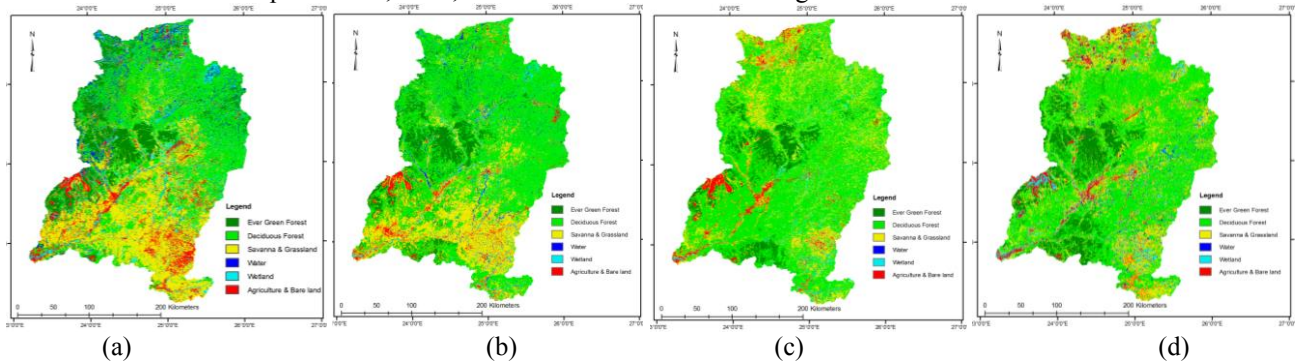

(a)   (b)   (c)   (d)

Figure 3. Land cover classifications for (a) 1984, (b) 1994, (c) 2001 and (d) 2009

Results of the accuracy assessment of classifying the 2009 image are shown in Table1. The Overall Accuracy was 88.58% with a Kappa Coefficient of 0.86 suggesting accurate classification. We note that a field survey is scheduled to collect ground control points to further improve classification results.

Table1. Confusion Matrix for 2009 LCC map

Class	Ground Truth						Prod Acc. (%)	User Acc. (%)
	EF	AG	WA	DF	SA	WL		
EF	208	2	0	2	0	0	76.75	98.11
AG	0	337	1	0	0	0	93.61	99.7
WA	0	0	216	0	1	12	91.14	94.32
DF	46	5	14	151	3	0	86.78	68.95
SA	17	8	5	21	185	19	97.37	72.55
WL	0	8	1	0	1	190	85.97	95

4.2 Trends in rainfall and stream flow

Fig. 4 shows the Mann-Kendall test statistics, of monthly and annual rainfall for stations at Mwinilunga, Solwezi, Zambezi and Kabompo.. Results indicate that in most of the period there is no significant trend in the rainfall. A significant decreasing trend, however, is detected in the months of April for Solwezi and Kabombo and an annual trend for Solwezi.
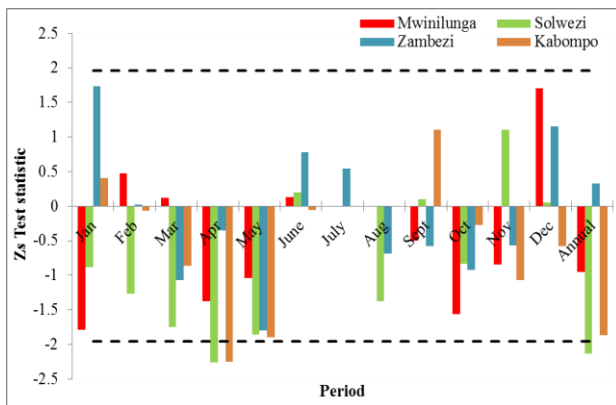

Figure 4. Individual Months and Annual Zs test statistic

The trend in the stream flow is shown in Fig. 5. Results indicate that for all months and for annual time series that trends are not statistically significant although an increasing trend is indicated.
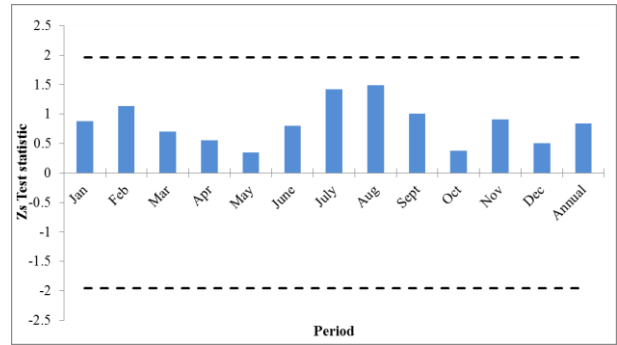

Figure 5. Individual Months and Annual Zs test statistic for stream flow
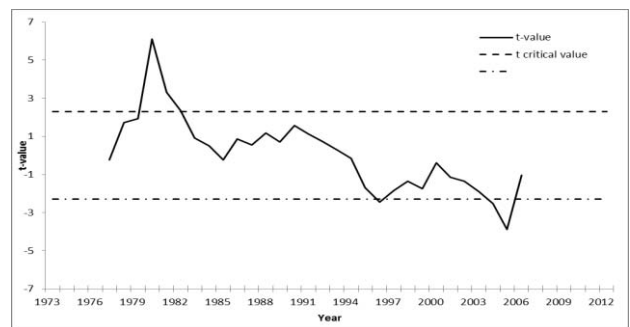
4.3 Change detection of stream flow

Figure 5. Change point detection for annual stream flow of Kabompo River at Watopa

The t-values are lower than the critical t-values for the years 1980, 1996 and 2005 (Fig.5). Periods for which changes occurred (i.e., change points) are for the periods 1973 to 1980, 1981 to 1996, 1997 to 2005 and 2005 to 2011. Satellite images for which land cover analysis is undertaken is available for 1984 and 1994 (covering period 1981 to 1996), 2001(covering period 1997 to 2005) and 2009 (covering period 2005 to 2011).

Table 2. Stream flow characteristics of Kabompo River Basin

	Time period			
	1973-1980	1981-1996	1997-2005	2006 - 2011
Annual flow (mm/ year)	133.24	82.66	105.66	144.03
High Flow Index(Q_5/Q_{50})	1.24	1.17	1.18	1.19
Low Flow Index(Q_{95}/Q_{50})	0.59	0.69	0.76	0.83

5. DISCUSSION AND CONCLUSION

The satalite images from the Landsat Surface Reflectance Climate Data were found to provide consistent atmospheric correction and were thus used for the systematic land cover classification.

The results from the trend analysis applied to rainfall time series indicate that some months exhibit an increasing trend while most months denote a decreasing trend. Most of the trends in the rainfall are not significant from a statistical point of view although they exhibit decreasing trend. Significant decreasing rainfall trend, however, was detected in the months of April for Solwezi and Kabombo and an annual trend for Solwezi. As expected in the dry season period (May to September), when there is virtually no rain there is no trend.

Four periods (1973 to 1980, 1981 to 1996, 1997 to 2005 and 2005 to 2011) have been identified in which changes occurred in the runoff regime.

The aim of this paper was to detect trends in rainfall and stream flow time series by means of statistical approaches and relating such trends with preliminary results on land cover changes. Preliminary results by this study show an increasing trend in stream flow whereas rainfall, in general, has a decreasing trend. This suggests that any change in runoff is not caused by changes in the climate. Changes in stream flow and hydrological catchment behaviour will be further investigated by applying the Soil and Water Assessment Tool (SWAT). The SWAT will be applied under the varying land cover types.

6. ACKNOWLEDGEMENTS

7. REFERENCES

1. Rientjes T. H. M., Haile A. T., Kebede E., Mannaerts C. M. M., Habib E. and Steenhuis T. S. (2011). *Changes in land cover, rainfall and stream flow in Upper Gilgel Abbay catchment, Blue Nile basin – Ethiopia.* Hydrol. Earth Syst. Sci., 15, 1979–1989.

2. World Bank, (2010). *The Zambezi River Basin. A Multi-Sector Investment Opportunities Analysis. Volume 3 State of the Basin.* Washington.

3. USGS, (2013). Landsat Missions. http://landsat.usgs.gov/LDCM_DataProduct.php

4. Lillesand, T.M. Kiefer, R.W. & Chipman, J.W. (2004). *Remote Sensing and Image Interpretation.* Fifth Edition.

5. Beyer, H. L. (2004). *Hawth's Analysis Tools for ArcGIS.* Available at http://www.spatialecology.com/htools

6. Foody, G. M. (2002). *Status of land cover classification accuracy assessment. Remote Sensing of Environment* 80(1): 185-201.

7. Helsel, D. R., and Hirsch, R. M. (2002). *Statistical methods in water resources*: U.S. Geological Survey Techniques of Water-Resources Investigations, Book 4, Chap. A3.

8. Helsel, D. R.; Hirsch, R. M. (1992). *Statistical Methods in Water Resources,* Studies in Environmental Science: Elsevier, Amsterdam, vol. 49.

9. Burkey, J. (2006). *A non-parametric monotonic trend test computing Mann-Kendall Tau, Tau-b, and Sens Slope written in Mathworks-MATLAB implemented using matrix rotations.* King County, Department of Natural Resources and Parks, Science and Technical Services section. Seattle, Washington. USA.

10. Cao M. S. (1998). *Detection of abrupt changes in glacier mass balance in the Tien Shan Mountains.* Journal of Glaciology, Vol. 44, No. 147, pp 352-358

11. Liang L., Li l., Liu Q. (2011). Precipitation variability in Northeast China from 1961 to 2008. Journal of Hydrology, Volume 404, Issues 1–2, Pages 67-76.

12. So, S. (2008). *Why is the sample variance a biased estimator?* https://maxwell.ict.griffith.edu.au/sso/biased_variance.pdf

13. McCuen, R. H. (2003). *Modeling Hydrologic Change: Statistical Method*s, CRC Press.

14. Davie, T. (2008). *Fundamentals of hydrology.* 2nd edition.